1. Theoretical Background

This chapter provides the background to interpret the dielectric function which is the quantity measured in THz spectroscopy. After an overview of the dynamics of charge carriers in optically excited metals, a model Hamiltonian describing a crystalline solid is introduced. This Hamiltonian is the basis for the rate equations governing the energy relaxation of excited electrons. Moreover, it is the starting point for a microscopic theory of the dielectric function. Finally, the case of a rapidly varying sample is discussed.

1.1. Ultrafast Processes in Optically Excited Metals

Since this work investigates the charge carrier dynamics in selected materials, it is useful to summarize the typical processes that electrons undergo after excitation by an ultrashort laser pulse. Here, the example of electrons in metals is chosen. Most of the following facts have been found by pump-probe techniques where an ultrashort laser pulse "pumps" charge carriers in the sample to excited states. The carriers are probed by a subsequent laser pulse, for instance by measuring the reflectivity of the sample or by photoemitting electrons whose kinetic energy is finally detected. The latter scheme is also called time-resolved photoelectron spectroscopy (TRPES).

The pump pulse with a duration of typically less than 100 fs and a photon energy of $\hbar\omega_{\mathrm{pump}} \sim 1\,\mathrm{eV}$ mainly interacts with the electrons of the system and couples their stationary quantum-mechanical states. As shown in the single-electron picture of Fig. 1.1(a), this leads to a polarization due to the superposition of single-electron eigenstates below and above the Fermi energy ϵ_{F}.

However, due to the interaction with the other electrons and the phonons, the phases between the superimposed stationary states are randomized on a time scale of 1 to 100 fs, and the system is left in a mixed state which is completely characterized by the occupation numbers of the eigenstates. In other words, the induced polarization has decayed, and the incident pump pulse has created electrons above ϵ_{F} and holes below ϵ_{F}, as illustrated in Fig. 1.1(b).

The above implies that the pump pulse energy is initially mainly deposited in the electronic system. Scattering processes exchange the energy among the excited and unexcited electrons and equilibrate to a Fermi-Dirac distribution which is characterized by an increased electronic temperature T_{e}. This electron thermalization takes place on a time scale of 10 to 1000 fs and is depicted in Fig. 1.1(c) [Hoh98].

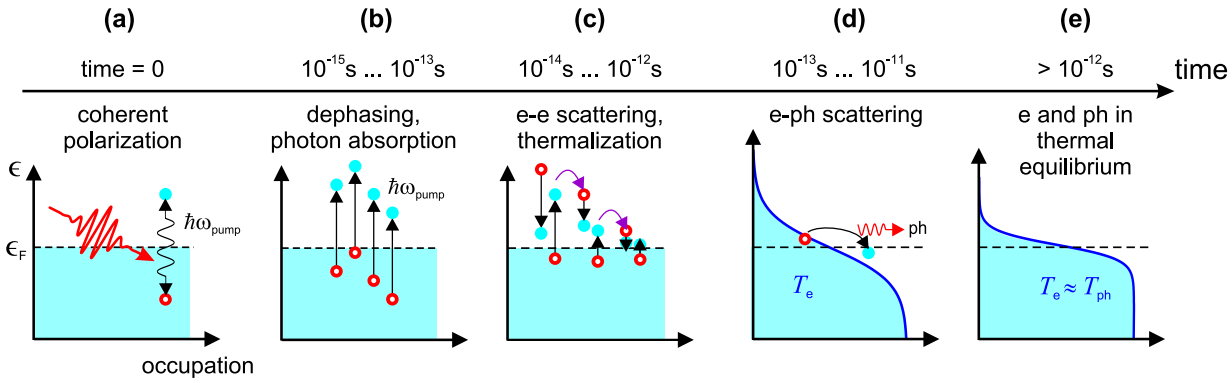

Figure 1.1.: Processes induced by a fs-laser pulse arriving at a metal surface. The metal is in thermal equilibrium before excitation. (a,b,c) After generation of a coherent polarization by the laser pulse and its decay, the excited electrons exchange energy with other electrons by electron-electron scattering. This thermalization finally leads to a Fermi-Dirac distribution of temperature T_e. (d) Directly after excitation, the electrons start to transfer energy to the cold lattice via electron-phonon coupling. The 2-temperature model becomes valid as soon as the electrons and phonons can be described by temperatures T_e and T_ph, respectively. (e) Finally, electrons and phonons arrive at the same temperature. Transport processes lead to energy dissipation in the considered volume, too.

The interaction between the lattice and the excited electrons leads to the emission of phonons and the cooling of the electrons on a time scale of 0.1 to 10 ps as seen in Fig. 1.1(d). In many cases, the resulting phonon population can be described by a Bose-Einstein distribution with phonon temperature T_ph, as for example in the 2-temperature model [Ani74]. However, this is not true in general, as shown for semiconductors [Els89] or the semimetal graphite in this work, where a non-equilibrium population of "hot phonons" is generated. The heat transfer from the electrons to the lattice fades as soon as electrons and phonons have arrived at the same temperature, $T_\mathrm{e} = T_\mathrm{ph}$, see Fig. 1.1(e).

It should be emphasized that all processes mentioned can temporally overlap. For example, the generation of phonons takes place already before the electrons have thermalized. Moreover, spatial transport processes set in from the very beginning. However, they can be neglected on these short time scales, if the pump pulse creates a homogeneously excited sample. On much longer time scales, heat diffusion leads to a cooling of the sample to the ambient temperature.

These mechanisms have important consequences in areas such as surface femtochemistry [Bon99]. For example, the hot electrons of laser-excited Ru were shown to trigger chemical reactions of adsorbed molecules that do not occur under equilibrium conditions [Bon99].

The dynamics of optically excited charge carriers in semiconductors and gases proceeds similarly to that in metals [Sha99]. Major differences concern the time scales involved and the recombination of electrons and holes which proceeds by phonon emission in metals. This is not possible in semiconductors where the phonon energies are much smaller than the band gap of $\sim$ 1 eV. Instead, photon emission, Auger and other processes lead to electron-hole recombination on a time scale of typically 1 ns. Long before, electrons and

holes thermalize to individual Fermi-Dirac distributions and equilibrate with the lattice by phonon emission.

The goal of this thesis is to study the dynamics of optically excited charge carriers in solids and gases by measuring the temporal evolution of its dielectric function in the far-infrared. The following sections give the theoretical background used in this work.

1.2. Model Hamiltonian of a Crystalline Solid

In the single-electron approach, the electrons in a solid are thought to move within a mean potential produced by the static lattice and the other electrons [Mad78]. The translational symmetry of a perfectly crystalline solid implies the Bloch theorem which states that the eigenstates of the single-electron Hamiltonian are Bloch states

$$|K\rangle = |\boldsymbol{k}B\rangle.$$

In real space, these states are plane waves modulated by the lattice-periodic Bloch factor u_K,

$$\langle \boldsymbol{x}|K\rangle = \exp(\mathrm{i}\boldsymbol{k}\boldsymbol{x})u_K(\boldsymbol{x}).$$

The quantum numbers involved are the wavevector $\boldsymbol{k}$, which is restricted to the 1st Brillouin zone (BZ), and the band index B, which also contains the spin degree of freedom. The corresponding single-electron eigenenergies ϵ_K constitute the band structure. When we neglect spin effects like ferromagnetism and spin-orbit coupling, ϵ_K will not depend on the spin, and the Bloch states factorize into an orbital and a spin part, $|K\rangle = |\boldsymbol{k}B\rangle = |\boldsymbol{k}b\rangle \otimes |\pm\rangle$ where $|\pm\rangle$ is the electronic spin-up and spin-down state, respectively. In the following, we mainly consider the orbital part $|k\rangle := |\boldsymbol{k}b\rangle$.

Phonons (ph) are the energy quanta $\hbar\Omega_Q$ of the fundamental lattice vibrations $Q = (\boldsymbol{q}, r)$ which are fully characterized by the phonon wavevector $\boldsymbol{q}$ and the phonon branch r; $\boldsymbol{q}$ is also restricted to the BZ.

The interaction between the lattice and the electrons can be understood as scattering an electron from state $|K\rangle$ into another state $|K'\rangle$,

$$|K\rangle \xrightarrow{\text{e-ph}} |K'\rangle,$$

accompanied by the annihilation $(+)$ and generation $(-)$ of phonons $Q^{\pm} = (\boldsymbol{q}^{\pm}, r)$, respectively. The matrix element $M^r_{K'K}$ of this process implies conservation of the total wavevector,

$$\boldsymbol{k}' = \boldsymbol{k} \pm \boldsymbol{q}^{\pm} + \boldsymbol{G},$$

where a reciprocal lattice vector $\boldsymbol{G}$ has to be added such that all wavevectors involved lie in the Brillouin zones. This can be abbreviated as

$$\boldsymbol{q}^{\pm} = [\pm(\boldsymbol{k}' - \boldsymbol{k})] \bmod \mathrm{BZ}.$$

So-called umklapp processes occur when $\boldsymbol{G} \neq 0$.

Electrons can also be scattered by impurities (imp) described by an impurity potential V^{imp}. Its matrix element $V^{\text{imp}}_{K'K} = \langle K'|V^{\text{imp}}|K\rangle$ quantifies the amplitude of this scattering process

$$|K\rangle \xrightarrow{\text{e-imp}} |K'\rangle.$$

With these definitions, the resulting model Hamiltonian of a crystalline solid can be written as [Nol01, Gri81, Mad78]

$$\hat{H} = \underbrace{\sum_{K} \epsilon_K \, \hat{a}^\dagger_K \hat{a}_K}_{\text{e in mean field}} + \underbrace{\sum_{Q} \hbar\Omega_Q \, \hat{b}^\dagger_Q \hat{b}_Q}_{\text{ph in mean field}} + \underbrace{\sum_{KK'r} M^r_{K'K} \, \hat{a}^\dagger_{K'} \hat{a}_K \left(\hat{b}_{\boldsymbol{q}^+ r} + \hat{b}^\dagger_{\boldsymbol{q}^- r}\right)}_{\text{e-ph coupling}} + \underbrace{\sum_{KK'} V^{\text{imp}}_{K'K} \, \hat{a}^\dagger_{K'} \hat{a}_K}_{\text{e-imp coupling}}. \tag{1.1}$$

Here, $\hat{a}^\dagger_K$ and $\hat{a}_K$ are operators creating and annihilating an electron in a state $|K\rangle$, respectively, whereas the operators $\hat{b}^\dagger_Q$ and $\hat{b}_Q$ do the same in the phonon subsystem. For example, e-ph coupling can be interpreted as the annihilation of an electron in state $|K\rangle$ and its creation in a new state $|K'\rangle$. This scattering process is induced by the generation or annihilation of a phonon $(\boldsymbol{q}^+, r)$ or $(\boldsymbol{q}^-, r)$, respectively. The e-ph interaction is screened by the surrounding mobile electrons and lattice ions.

Electron-electron interaction is neglected here, since it is already mainly contained in the Bloch states and the band structure.

1.3. Population Dynamics and 2-Temperature Model

1.3.1. Rate Equations

The dynamics of a solid are rigorously described by the evolution of its total density matrix which is extremely complicated to calculate for a many-body system. Therefore, the dynamics is often modeled by rate equations which only take the population of the stationary states, that is the diagonal elements of the density matrix, into account. The population then changes due to transitions between stationary states, and the transition probabilities are calculated by Fermi's Golden Rule which implies strict conservation of energy. This is, however, not true any more on short time scales where time-energy uncertainty starts to play a role. Such effects have been observed in the energy relaxation of electrons by phonon emission in GaAs [Für96].

Within a single-particle picture, the population is given by the occupation numbers f_k and b_Q of electronic Bloch states $|k\rangle$ and lattice vibrational modes Q, respectively. The resulting rate equation for the electronic population is [Mad78, All87, Gri81]

$$\frac{\partial f_k}{\partial t} = \sum_{k'} \left[w_{k'k} \cdot f_{k'} \cdot (1 - f_k) - w_{kk'} \cdot f_k \cdot (1 - f_{k'})\right] \tag{1.2}$$

where the 2 terms describe the scattering into $|k\rangle$ and out of $|k\rangle$, respectively. The transition rates $w_{kk'}$ for e-ph scattering involve both phonon generation ($-$) and annihilation ($+$),

$$w_{kk'}^{\text{e-ph}} = \frac{2\pi}{\hbar} \sum_{r,\pm} |M_{k'k}^{r}|^2 \left(b_{Q^\pm} + \tfrac{1}{2} \pm \tfrac{1}{2}\right) \delta\left(\epsilon_{k'} - \epsilon_k \pm \hbar\Omega_{Q^\pm}\right). \tag{1.3}$$

The annihilation rate of phonons $Q^+ = (\boldsymbol{q}^+, r)$ grows linearly with their occupation number b_{Q^+} whereas the generation rate is proportional to $b_{Q^-} + 1$ since also "spontaneous emission" of phonons $Q^- = (\boldsymbol{q}^-, r)$ can occur for $b_{Q^-} = 0$. The δ-functions enforce energy conservation in an e-ph scattering process.

Electron-impurity and e-e scattering give corresponding contributions to this rate equation [Mad78]. Especially, in case of a real (not complex) impurity potential, e-imp scattering is elastic and does not change the energy of the involved electron. In addition, the optical excitation of the metal can also be described by a term analog to (1.3).

The rate equation for the phonon distribution b_Q is very similar but with a contribution from ph-ph scattering instead of e-e scattering which originates from the anharmonic coupling between the normal lattice vibrations Q. It is responsible for the energy redistribution within the phonon system.

It should be noted that the rate equation (1.2) does not take transport effects into account.

1.3.2. 2-Temperature Model for Metals

In order to simplify the rate equations, the 2-temperature model (2TM) describes the electrons and phonons by merely 2 temperatures:

- The electrons are assumed to be thermalized at any time and thus to follow a Fermi-Dirac distribution
$$f(\epsilon) = \frac{1}{\exp(\beta_\text{e}\epsilon - \beta_\text{e}\mu) + 1} \tag{1.4}$$
with temperature $T_\text{e} = 1/k_\text{B}\beta_\text{e}$ and chemical potential μ. The electron occupation numbers are then $f_K = f(\epsilon_K)$. The reason for this assumption is that the e-e interaction is usually stronger than the e-ph interaction. Therefore, the electron subsystem thermalizes before the thermal equilibrium between electrons and phonons is established. As a consequence, e-e and e-imp scattering can be neglected in the rate equations.

- Similarly, the phonons are assumed to follow a Bose-Einstein distribution
$$b(\Omega) = \frac{1}{\exp(\beta_\text{ph}\hbar\Omega) - 1} \tag{1.5}$$
with temperature $T_\text{ph} = 1/k_\text{B}\beta_\text{ph}$. The phonon occupation numbers are then $b_Q = b(\Omega_Q)$. This assumption can be easily violated in semiconductors [Els89] or semimetals as shown in Chapter 4 for graphite.

The total energy of the electron subsystem is

$$E_\mathrm{e} = 2\sum_k f_k \epsilon_k$$

where the factor of 2 is due to the spin degeneracy. Its temporal change can be calculated with the aid of Eqs. (1.2) and (1.3). Since the occupation numbers only depend on energy, $f_k = f(\epsilon_k)$ and $b_Q = b(\Omega_Q)$, one obtains an integral over the initial electron energy ϵ, final electron energy ϵ', and phonon frequency Ω [All87],

$$\frac{\partial E_\mathrm{e}}{\partial t} = 4\pi \iiint \mathrm{d}\epsilon\, \mathrm{d}\epsilon'\, \mathrm{d}\Omega\, S(\epsilon, \epsilon', \Omega)\, \Omega\, \delta(\epsilon' - \epsilon - \hbar\Omega)\, H(\epsilon, \epsilon', \Omega). \tag{1.6}$$

Here,

$$S(\epsilon, \epsilon', \Omega) = [f(\epsilon) - f(\epsilon')]b(\Omega) - [1 - f(\epsilon)]f(\epsilon')$$

embraces all occupation numbers. The auxiliary function

$$H(\epsilon, \epsilon', \Omega) = \sum_{kk'r} |M^r_{k'k}|^2 \delta(\epsilon - \epsilon_k)\delta(\epsilon' - \epsilon_{k'})\delta(\Omega - \Omega_Q)$$

is proportional to the Eliashberg function $\alpha^2F(\epsilon, \epsilon', \Omega)$ which contains all necessary information on e-ph interaction [Gri81, All87].

Sources of the electronic energy such as the exciting laser pulse have to be added on the right-hand side of Eq. (1.6). As mentioned before, transport effects are neglected.

Most electronic transitions of interest occur around the Fermi edge. In metals, the electronic density of states (eDOS)

$$D(\epsilon) = 2\sum_k \delta(\epsilon - \epsilon_k) \tag{1.7}$$

shows only small relative variations there such that α^2F is usually evaluated at $\epsilon = \epsilon' = \epsilon_\mathrm{F}$. However, this is not possible for the semimetal graphite where we have to take the strongly varying eDOS into account.

1.4. What Is Measured in an Optical Experiment?

The dielectric function of a sample is the central quantity that is measured in THz spectroscopy. The following sections give a definition of the dielectric function and its relation to the microscopic properties of the sample.

1.4.1. Induced Electric Polarization

In a typical optical experiment, a light wave is incident on a sample, partially transmitted, and finally detected. Inside the sample, the *electric* field $\boldsymbol{E}$ of the light wave modifies the charge distribution and thus induces an electric polarization $\boldsymbol{P}$ or, equivalently, an electric current density

$$\boldsymbol{j}_{\mathrm{ind}} = \frac{\partial \boldsymbol{P}}{\partial t}. \tag{1.8}$$

This in turn alters the total electric field $\boldsymbol{E}$ and makes wave propagation in matter different from that in vacuum. Detecting the transmitted light wave therefore means measuring how easily the light field can polarize the sample or, equivalently, how easily it can induce an electric current. This ease is quantified by the so-called dielectric function and can be determined by THz spectroscopy.

Before turning to the formal relation between electric field, induced polarization, and dielectric function, it is worth mentioning the following points:

- The material response to the *magnetic* component of the electromagnetic field is largely negligible at THz and higher frequencies since the magnetic dipoles within the material cannot follow the fast magnetic field oscillations [Mil98]. An exception are so-called optical metamaterials. In these arrays of small LC oscillators, magnetic effects can become important at THz frequencies [Lin04].

- Most theories consider only macroscopic fields $\boldsymbol{E}$ and $\boldsymbol{P}$ which are the true microscopic fields averaged over a length l_{avg}. In this way, one gets rid of all variations on length scales much smaller than the characteristic length l_{opt} of the electromagnetic wave where l_{opt} can be its wavelength λ or attenuation length. Therefore, l_{avg} should be well below l_{opt} but large compared to the length scale l_{mat} on which the microscopic electric field varies in the unperturbed matter. In a solid one typically has $l_{\mathrm{mat}} \sim 1\,\text{Å}$ and $l_{\mathrm{opt}} \sim \lambda \sim 100\,\mathrm{nm}$ at optical frequencies. In this case, the choice $l_{\mathrm{avg}} \sim 10\,\mathrm{nm}$ surely fulfills the condition $l_{\mathrm{mat}} \ll l_{\mathrm{avg}} \ll l_{\mathrm{opt}}$.

1.4.2. Dielectric Function ε

How is $\boldsymbol{P}$ related to the intrinsic properties of the sample? In general, it will depend on the electric field $\boldsymbol{E}$ in a complicated manner. Fortunately, the strength $\sim e/(1\,\text{Å})^2 \sim 10^9\,\mathrm{V\,cm^{-1}}$ of the microscopic fields in unperturbed matter is often much larger than $\boldsymbol{E}$. In this case, $\boldsymbol{P}$ can be expanded in a power series with respect to $\boldsymbol{E}$,

$$\boldsymbol{P}(\boldsymbol{E}) = \boldsymbol{P}^{(1)} + \boldsymbol{P}^{(2)} + \ldots, \tag{1.9}$$

where $\boldsymbol{P}^{(j)}$ is of exactly jth order in $\boldsymbol{E}$. This series is sometimes called a Volterra series since the expansion argument is not a number but a complete function $\boldsymbol{E}(\boldsymbol{x}, t)$ [Gra78]. The

leading term $\boldsymbol{P}^{(0)}$ is zero since a vanishing macroscopic field does not induce a polarization at THz and higher frequencies. In the following we assume that $\boldsymbol{E}$ induces only a spatially localized polarization $\boldsymbol{P}$. In other words, $\boldsymbol{E}(\boldsymbol{x}, t)$ induces a coherent polarization within a radius around $\boldsymbol{x}$ that is much smaller than l_{opt} [Mil98]. In contrast, the polarization response is temporally nonlocal in general, that is the complete past of the electric field affects the polarization at time t.

In case the sample is in a steady state, one can switch from the time domain to frequency space by a Fourier transformation where the linear response becomes simply

$$\boldsymbol{P}^{(1)}(\boldsymbol{x}, \omega) = \chi(\boldsymbol{x}, \omega)\boldsymbol{E}(\boldsymbol{x}, \omega). \tag{1.10}$$

The 2nd-rank tensor $\chi(\boldsymbol{x}, \omega)$ is called the linear susceptibility at angular frequency ω which reduces to a scalar in a locally isotropic medium. The dielectric function ε, the conductivity σ, and the refractive index n are often used instead of χ. They contain the same amount of information and are defined in ω space by

$$\varepsilon = 1 + 4\pi\chi, \quad \sigma = -\mathrm{i}\omega\chi = \frac{\omega}{4\pi\mathrm{i}}(\varepsilon - 1), \quad \text{and} \quad n = \sqrt{\varepsilon},$$

respectively. ε and χ will be used equally in this work. By using Eq. (1.8), the term "conductivity" becomes clear from its relation to the induced current,

$$\boldsymbol{j}_{\text{ind}}^{(1)}(\boldsymbol{x}, \omega) = \sigma(\boldsymbol{x}, \omega)\boldsymbol{E}(\boldsymbol{x}, \omega).$$

The relation between the dielectric function and the microscopic structure of the sample will be discussed in the following section.

A simple macroscopic interpretation can be at least given for the imaginary part of the dielectric function: It describes how efficiently the medium can absorb light. According to Poynting's theorem, the temporally averaged power $\mathrm{d}P_{\text{abs}}$ absorbed from a monochromatic light wave $\boldsymbol{E}(\boldsymbol{x}, t) = \mathrm{Re}\,[\boldsymbol{A}(\boldsymbol{x})\exp(\mathrm{i}\omega t)]$ in a volume $\mathrm{d}V$ around point $\boldsymbol{x}$ is [Röm94]

$$\frac{\mathrm{d}P_{\text{abs}}}{\mathrm{d}V} = \left\langle \boldsymbol{E}\frac{\partial \boldsymbol{P}}{\partial t} \right\rangle = \frac{1}{2}\omega|\boldsymbol{A}|^2\,\mathrm{Im}\,\varepsilon(\boldsymbol{x}, \omega),$$

where the medium is assumed to be optically isotropic. The real part of the dielectric function is connected to its imaginary part by the Kramers-Kronig relations which are a direct consequence of causality [Röm94].

Due to the knowledge of the electric field of the probing pulse, THz spectroscopy allows to measure the dielectric function of a sample, which is the ultimate goal of linear optical spectroscopy. In TRTS, the sample is excited by a pump pulse, and one can even monitor the evolution of the dielectric function as a function of the delay between pump and THz probe pulse. It is, therefore, desirable to know the relation between the dielectric function and the microscopic properties of the sample. This issue is discussed in the next sections using classical models and a more rigorous quantum-theoretical description.

1.5. Microscopic Models for ε

1.5.1. Classical Models

Bound Electrons: Lorentz Oscillator

In the Lorentz model, a bound particle j with charge q and mass m is located in the minimum position of some potential. The light field $\boldsymbol{E}$ acts on the charge as a small perturbation and, within the dipole approximation, leads to a harmonic oscillation $\boldsymbol{x}_j(t)$ with resonance frequency ω_0 and damping rate γ around the potential minimum at $\boldsymbol{x}_{0j}$. The dipole moment induced by the oscillating charge is $\boldsymbol{p}_j = q \cdot (\boldsymbol{x}_j - \boldsymbol{x}_{0j})$, and the macroscopic polarization is the sum of all N dipoles per averaging volume $V_{\mathrm{avg}} = l_{\mathrm{avg}}^3$ around position $\boldsymbol{x}$. In ω space, this yields

$$\boldsymbol{P}(\boldsymbol{x},\omega) = \frac{1}{V_{\mathrm{avg}}} \sum_{j=1}^{N} \boldsymbol{p}_j = \frac{\varepsilon^{\mathrm{Lorentz}} - 1}{4\pi} \boldsymbol{E}(\boldsymbol{x},\omega)$$

with the dielectric function

$$\varepsilon^{\mathrm{Lorentz}}(\omega) = 1 + \frac{4\pi N q^2}{V_{\mathrm{avg}} m} \frac{1}{\omega_0^2 - \omega^2 - \mathrm{i}\gamma\omega}. \tag{1.11}$$

Equation (1.11) exhibits a resonance denominator such that $\operatorname{Im} \varepsilon^{\mathrm{Lorentz}}(\omega)$ and the absorption of light peak at $\omega = \omega_0$ in case of small damping, $\gamma \ll \omega$. Although based on classical mechanics, the Lorentz model describes the optical response of molecular vibrations and phonons quite well [Ash76].

Free Electrons: Drude Model

The Lorentz model contains also the limiting case $\omega_0 = 0$ of free or unbound electrons which yields the Drude formula

$$\varepsilon^{\mathrm{Drude}}(\omega) = 1 - \frac{\Omega_{\mathrm{pl}}^2}{\omega^2 + \mathrm{i}\Gamma\omega} \tag{1.12}$$

with squared plasma frequency

$$\Omega_{\mathrm{pl}}^2 = \frac{4\pi n_{\mathrm{e}} e^2}{m_{\mathrm{e}}} \tag{1.13}$$

and free-electron density n_{e}. The damping rate Γ can be interpreted more explicitly when the damping of the electron oscillation is caused by collisions of the electron with obstacles. If each collision completely randomizes the electron velocity, $1/\Gamma$ is just the time between 2 subsequent collisions. In other words, $1/\Gamma$ is the characteristic time it takes to relax an electronic current when the driving electric field is switched off [Ash76].

Although the Drude formula is based on an extremely simplified model, it often provides a good *phenomenological* description of the optical properties of metals and doped semiconductors. As will be discussed below, it can be derived under certain assumptions from more sophisticated models.

1.5.2. Semiclassical Theory: Boltzmann Equation

In a semiclassical approach and in a spatially homogeneous system, the electrons can be described by a distribution function $f(\boldsymbol{v}, t)$ where $f(\boldsymbol{v}, t)\,\mathrm{d}^3\boldsymbol{v}$ is the density of electrons having their velocity in the interval $[\boldsymbol{v}, \boldsymbol{v} + \mathrm{d}\boldsymbol{v}]$. The dynamics of f in a homogeneous external electric field $\boldsymbol{E}$ is described by the Boltzmann equation [Hol65]

$$\frac{\partial f}{\partial t} - \frac{e}{m_\mathrm{e}} \frac{\partial f}{\partial \boldsymbol{v}} \boldsymbol{E} = \left.\frac{\partial f}{\partial t}\right|_\mathrm{scatt}.$$

The term on the right-hand side describes scattering events between the electrons and other obstacles which can change the velocity $\boldsymbol{v}$ of an electron and therefore lead to a redistribution of $f(\boldsymbol{v}, t)$. In case of a vanishing electric field, thermalization by electron-electron scattering results in the familiar Maxwell-Boltzmann distribution

$$f(\boldsymbol{v}, t) = n_\mathrm{e} \left(\frac{m_\mathrm{e}}{2\pi k_\mathrm{B} T_\mathrm{e}}\right)^{3/2} \exp\left(-\frac{m_\mathrm{e}\boldsymbol{v}^2}{2k_\mathrm{B} T_\mathrm{e}}\right), \tag{1.14}$$

with electronic temperature T_e.

An external electric field $\boldsymbol{E}$ modifies this distribution and induces an electric current. By treating $\boldsymbol{E}$ as a weak perturbation and assuming that the electrons undergo only *binary* collisions with much heavier obstacles such as ions or neutral particles, one can derive the dielectric function of such a system [Hol65],

$$\varepsilon^\mathrm{Boltzmann}(\omega) = 1 + \frac{(4\pi e)^2}{3 m_\mathrm{e} \omega} \int_0^\infty \mathrm{d}v\, \frac{\partial f}{\partial v} v^3\, \frac{1}{\omega + \mathrm{i}\gamma(v)}. \tag{1.15}$$

Here,

$$\gamma(v) = \sum_j v n_j \sigma_{\mathrm{e}j} \tag{1.16}$$

is the collision rate of an electron having velocity $v = |\boldsymbol{v}|$ caused by scattering off all sorts j of obstacles. Each obstacle species j is characterized by a density n_j and a momentum-transfer cross section $\sigma_{\mathrm{e}j}$ for scattering with electrons.

Note that electrons with a velocity around a fixed value v make a Drude-like contribution to the integration in Eq. (1.15). Moreover, if the collision rate $\gamma(v)$ does not depend on the electron velocity v, one can show, that Eq. (1.15) reduces exactly to the Drude formula (1.12) with electron density $n_\mathrm{e} = \int \mathrm{d}^3\boldsymbol{v}\, f$ [Hol65].

It should be mentioned that the relation (1.15) does not account for e-e scattering. Quantum effects can be included in Eq. (1.15) by calculating the cross sections $\sigma_{\mathrm{e}j}$ according to quantum mechanics and by using the Fermi-Dirac distribution (1.4) instead of the Maxwell-Boltzmann distribution [Mad78].

1.5.3. Quantum-Mechanical Theory: Kubo Formula

Assume that only the electrons of some system interact with a classical light wave given by the vector potential $\boldsymbol{A}(\boldsymbol{x},t)$. Then, to 1st order in the light field and in Coulomb gauge, this interaction is described by the Hamiltonian [Czy04]

$$\hat{H}_{\text{e-light}} = -\frac{1}{c}\int \mathrm{d}^3\boldsymbol{x}\,\hat{\boldsymbol{j}}(\boldsymbol{x})\boldsymbol{A}(\hat{\boldsymbol{x}},t).$$

where the operator of the electronic current density

$$\hat{\boldsymbol{j}}(\boldsymbol{x}) = -\frac{e}{2m_{\mathrm{e}}}\sum_j [\hat{\boldsymbol{\pi}}_j\delta(\boldsymbol{x}-\hat{\boldsymbol{x}}_j) + \delta(\boldsymbol{x}-\hat{\boldsymbol{x}}_j)\hat{\boldsymbol{\pi}}_j]$$

contains position $\hat{\boldsymbol{x}}_j$ and canonical momentum $\hat{\boldsymbol{\pi}}_j$ of all electrons labeled j. Application of 1st-order perturbation theory in $\hat{H}_{\text{e-light}}$ yields the Kubo formula for the tensor of the dielectric function [Czy04],

$$\varepsilon_{\alpha\beta}^{\text{Kubo}}(\omega) = -\frac{4\pi n_{\mathrm{e}}e^2}{m_{\mathrm{e}}\omega^2} + \frac{4\pi}{V\omega^2}\sum_{mm'}\frac{\langle m'|\hat{j}_\alpha|m\rangle\langle m|\hat{j}_\beta|m'\rangle}{E_{m'}-E_m-\hbar\omega-\mathrm{i}0^+}(\rho_{mm}-\rho_{m'm'}). \tag{1.17}$$

In this expression, one has to sum over all initial and final eigenstates $|m\rangle$ and $|m'\rangle$ of the unperturbed system, respectively. Light with frequency ω is absorbed if the photon energy $\hbar\omega$ matches the difference between 2 eigenenergies $E_{m'}$ and E_m and if the population ρ_{mm} of the initial state exceeds the population $\rho_{m'm'}$ of the final state. The infinitesimally small positive number 0^+ ensures that the perturbing electric field $\boldsymbol{E}$ is off in the far past.

The derivation of this formula involves the dipole approximation and therefore leads to a spatially local response. It moreover neglects the off-diagonal elements $\rho_{mm'}$ of the density matrix, that is any coherences in the unperturbed system. Finally, the derivation assumes the unperturbed system to change slowly within 1 cycle $2\pi/\omega$ of the probing light field. This point will be discussed in Section 1.8.

It should be mentioned that the Kubo formula can be rewritten in terms of fluctuations of the current density which leads to a version of the fluctuation-dissipation theorem: Photon absorption is related to fluctuations of the current density in the *unperturbed* system [McQ76].

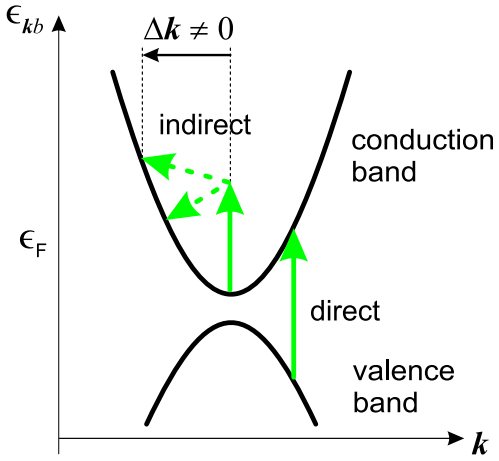

Figure 1.2.: Photon absorption by *resonant* direct and indirect optical transitions of Bloch electrons. Direct transitions conserve the electron wavevector and appear as vertical arrows in the band structure. Indirect optical transitions, in contrast, involve an additional wavevector source and appear as nonvertical arrows.

1.5.4. Local Electric Field

All models for the dielectric function presented up to here tacitly assume that the total macroscopic field $\boldsymbol{E}$ perturbs the motion of the electrons. Strictly speaking, one has to consider the local electric field $\boldsymbol{E}_{\mathrm{loc}}(\boldsymbol{x}, t)$ which is the total electric field acting on a charge at position $\boldsymbol{x}$ [Adl62].

Although the local field does generally not equal the macroscopic field one usually neglects local-field effects by setting $\boldsymbol{E}_{\mathrm{loc}} = \boldsymbol{E}$. This can lead to significant discrepancies between modeled and calculated dielectric function [Yu99].

1.6. Optical Transitions in Crystalline Solids

In the following, the Kubo formula is considered for the Bloch electrons of a crystalline solid. As seen above, the absorption of a photon is possible by a transition $|m\rangle \rightarrow |m'\rangle$ between eigenstates of the unperturbed system. Application of the Kubo formula to the model Hamiltonian (1.1) shows, that 2 distinct classes of optical transitions $|\boldsymbol{k}b\rangle \rightarrow |\boldsymbol{k}'b'\rangle$ between electronic Bloch states contribute to the linear optical response of a crystalline solid [Bas75]:

1. A *direct* optical transition (DOT) only involves the interaction between Bloch electrons and the light field; the influence of lattice imperfections is neglected. In a DOT, the electron wavevector remains nearly unchanged, $\Delta\boldsymbol{k} = 0$, since the wavevector of the light field is much smaller than the linear dimensions of the BZ. Therefore, photon absorption by a DOT corresponds to a resonant *vertical* transition in the band structure as illustrated in Fig. 1.2.

2. An *indirect* optical transition (IOT) is a higher-order process since it involves the interaction between Bloch electrons, the light field, and lattice imperfections like

impurities and phonons. It generally implies changes in the electronic wavevector, $\Delta\boldsymbol{k} \neq 0$. Photon absorption by an IOT corresponds to a resonant *nonvertical* transition in the band structure as shown in Fig. 1.2.

In the following, DOTs and IOTs are explained in more detail and compared to the classical Drude model. For this purpose, the Drude formula (1.12) is linearized in Γ resulting in

$$\varepsilon^{\mathrm{Drude}} = 1 - \frac{\Omega_{\mathrm{pl}}^2}{\omega^2} + \mathrm{i}\frac{\Omega_{\mathrm{pl}}^2}{\omega^3}\Gamma. \tag{1.18}$$

It will turn out that $\operatorname{Re}\varepsilon^{\mathrm{Drude}}$ can be assigned to direct intraband transitions (intraDOTs), whereas the dissipative part $\operatorname{Im}\varepsilon^{\mathrm{Drude}}$ of the Drude formula can be associated with IOTs, that is

$$\varepsilon^{\mathrm{Drude}} = \varepsilon^{\mathrm{intraDOT}} + \mathrm{i}\operatorname{Im}\varepsilon^{\mathrm{IOT}}.$$

1.6.1. Direct Optical Transitions

As described above, direct optical transitions conserve the electron wavevector, and the transition is therefore

$$|\boldsymbol{k}b\rangle \xrightarrow{\text{photon}} |\boldsymbol{k}b'\rangle.$$

It is useful to separate the DOTs in interband ($b \neq b'$) and intraband ($b = b'$) transitions,

$$\varepsilon^{\mathrm{DOT}} = \varepsilon^{\mathrm{interDOT}} + \varepsilon^{\mathrm{intraDOT}}.$$

The diagonal elements of the *interband* part are [Ped03]

$$\varepsilon_{\alpha\alpha}^{\mathrm{interDOT}} = \frac{2\cdot 4\pi e^2\hbar^2}{m_{\mathrm{e}}^2 V} \sum_{\substack{bb'\boldsymbol{k}\\ b\neq b'}} \frac{|\langle b'\boldsymbol{k}|\hat{\pi}_\alpha|b\boldsymbol{k}\rangle|^2\,(f_{b'\boldsymbol{k}} - f_{b\boldsymbol{k}})}{(\epsilon_{b'\boldsymbol{k}} - \epsilon_{b\boldsymbol{k}})^2\,(\epsilon_{b'\boldsymbol{k}} - \epsilon_{b\boldsymbol{k}} - \hbar\omega - \mathrm{i}0^+)} \tag{1.19}$$

where V is the volume of the system. The factor of 2 accounts for the electron spin which is conserved in the transitions considered due to $\langle +|-\rangle = 0$. Similar to the Kubo formula, the resonance denominator enables light absorption if the photon energy $\hbar\omega$ matches an energy difference $\epsilon_{\boldsymbol{k}b'} - \epsilon_{\boldsymbol{k}b}$.

If the occupation numbers depend only on the electron energy, $f_k = f(\epsilon_k)$, the *intraband* part of $\varepsilon^{\mathrm{DOT}}$ is [Ped03]

$$\varepsilon^{\mathrm{intraDOT}} = 1 + \frac{1}{\omega^2}\frac{2\cdot 4\pi e^2}{V}\sum_k \left.\frac{\partial f}{\partial\epsilon}\right|_k \boldsymbol{v}_k{}^{\mathrm{t}}\boldsymbol{v}_k$$

with $\boldsymbol{v}_k$ being the band velocity

$$\boldsymbol{v}_k = \frac{1}{\hbar}\frac{\partial\epsilon_k}{\partial\boldsymbol{k}}. \tag{1.20}$$

Since an intraDOT has vanishing transition energy its contribution to the optical response is often called *free-carrier response*. It becomes appreciable for a large eDOS and large band velocities around the Fermi edge where $\partial f/\partial\epsilon \neq 0$. The intraDOTs are a nonresonant contribution, affect only the real part of the dielectric function, and result in a negative $\mathrm{Re}\,\varepsilon_{\alpha\alpha}^{\mathrm{intraDOT}}$ with a typical $1/\omega^2$ dependence.

Due to these properties, intraDOTs resemble the situation of the collisionless Drude model. This becomes even more apparent for the case of quasifree electrons with effective mass m_{eff} and density n_{e}. They are described by 1 parabolic band

$$\epsilon_{\boldsymbol{k}} = \frac{\hbar^2}{2m_{\mathrm{eff}}}\boldsymbol{k}^2$$

which implies a band velocity proportional to their wavevector,

$$\boldsymbol{v}_{\boldsymbol{k}} = \frac{\hbar}{m_{\mathrm{eff}}}\boldsymbol{k}. \tag{1.21}$$

Such situation occurs, for example, in several metals like Na [Ash76] or in doped semiconductors like n-GaAs or n-InAs [Els89]. Provided the band is not completely filled or empty, one obtains a scalar dielectric function $\varepsilon^{\mathrm{intraDOT}} = 1 - 4\pi e^2 n_{\mathrm{e}}/|m_{\mathrm{eff}}|\omega^2$, just like in the collisionless Drude model.

This striking analogy and Eq. (1.18) lead to a generalized definition of the *free-carrier plasma frequency*

$$\Omega_{\mathrm{pl}}^2 = -\frac{8\pi e^2}{V}\sum_k \left.\frac{\partial f}{\partial\epsilon}\right|_k \boldsymbol{v}_k{}^{\mathrm{t}}\boldsymbol{v}_k = -\frac{8\pi e^2}{V}\int \mathrm{d}\epsilon\,\frac{\partial f}{\partial\epsilon}\,v^2 D(\epsilon). \tag{1.22}$$

Here, the velocity-weighted eDOS

$$v^2 D(\epsilon) = \sum_k \boldsymbol{v}_k{}^{\mathrm{t}}\boldsymbol{v}_k\,\delta(\epsilon - \epsilon_k) \tag{1.23}$$

has roughly the same spectral structure like the ordinary eDOS $D(\epsilon)$ of Eq. (1.7) [All71]. Note that Ω_{pl}^2 is a 2nd-rank tensor which is diagonal in an appropriately chosen coordinate system.

Metals usually exhibit a large and nearly constant eDOS around the Fermi edge. Then one can set $\epsilon = \epsilon_{\mathrm{F}}$ in Eq. (1.22), which makes the plasma frequency independent of the electron distribution $f(\epsilon)$. Assuming moreover a constant band velocity $v_{k\alpha}^2 = v_{\mathrm{F}}^2/3$ provides the estimate

$$\Omega_{\mathrm{pl}\alpha\alpha}^2 \sim \frac{4}{3}\pi e^2 v_{\mathrm{F}}^2 \frac{D(\epsilon_{\mathrm{F}})}{V},$$

where D is the eDOS, and v_{F} can be interpreted as the electron band velocity averaged over the Fermi surface.

1.6.2. Indirect Optical Transitions

The effect of lattice imperfections like impurities or phonons on the optical response is now taken into account to lowest nonvanishing order. The resulting summation over the IOTs

$$|k\rangle = |\boldsymbol{k}b\rangle \xrightarrow{\text{photon}} |k''\rangle = |\boldsymbol{k}b''\rangle \xrightarrow{\text{ph, imp}} |k'\rangle = |\boldsymbol{k}'b'\rangle$$

makes an additional contribution only to the imaginary part of the dielectric function as is exactly the case in the linearized Drude formula (1.18). One obtains [vB72][1]

$$\operatorname{Im}\varepsilon_{\alpha\alpha}^{\text{IOT}} = \frac{2(2\pi\hbar e)^2}{(\hbar\omega)^4 V}\sum_{kk'} w_{kk'\omega}\cdot(v_{k\alpha}-v_{k'\alpha})^2\, f_k\cdot(1-f_{k'}) \tag{1.24}$$

where the electron transition rate due to electron-impurity-photon and electron-phonon-photon coupling is

$$w_{kk'\omega}^{\text{e-imp}} = |V_{k'k}^{\text{imp}}|^2\cdot[\delta(\epsilon_{k'}-\epsilon_k-\hbar\omega)-\delta(\epsilon_{k'}-\epsilon_k+\hbar\omega)]$$

and

$$w_{kk'\omega}^{\text{e-ph}} = \sum_{r\pm}|M_{k'k}^{r}|^2\left(b_{Q^\pm}+\tfrac{1}{2}\pm\tfrac{1}{2}\right)[\delta(\epsilon_{k'}-\epsilon_k\pm\hbar\Omega_{Q^\pm}-\hbar\omega)-\delta(\epsilon_{k'}-\epsilon_k\pm\hbar\Omega_{Q^\pm}+\hbar\omega)], \tag{1.25}$$

respectively. In this formalism, the lattice imperfections scatter the more electrons from $|k\rangle$ to $|k'\rangle$ the more electrons are in the initial state and the less electrons are in the final state. However, as suggested by Eq. (1.24), absorption of light being polarized along the α direction only occurs if the electron changes its band velocity $v_{k\alpha}$ along the same direction $\alpha\in\{x,y,z\}$.

This situation again is quite similar to that of the Drude model and together with Eq. (1.18) motivates the definition of a generalized *Drude scattering rate* [All71]

$$\Gamma(\omega) = \frac{\omega^3}{\Omega_{\text{pl}\alpha\alpha}^2}\operatorname{Im}\varepsilon_{\alpha\alpha}^{\text{IOT}}. \tag{1.26}$$

Assuming a constant band velocity $v_{k\alpha}^2 = v_{\text{F}}^2/3$, constant matrix elements $|V_{kk'}^{\text{imp}}|^2 = |V_{\text{F}}^{\text{imp}}|^2$ for impurity scattering, and a constant eDOS D around the Fermi edge yields an estimate

$$\Gamma^{\text{imp}} \sim \frac{\pi}{\hbar}|V_{\text{F}}^{\text{imp}}|^2 D(\epsilon_{\text{F}}) \tag{1.27}$$

for the Drude scattering rate where v_{F} and $|V_{\text{F}}^{\text{imp}}|^2$ can be understood as averages over the Fermi surface. A large eDOS $D(\epsilon_{\text{F}})$ implies many initial and final states for scattering electrons and thus leads to a large velocity-relaxation rate.

In general, Γ has to be calculated according to Eqs. (1.24) and (1.26) and thus depends on temperature and light frequency which is especially relevant for a strongly varying eDOS around the Fermi energy and for e-ph scattering.

[1] This formula is also derived in [All71] for low temperatures. Note that a factor of $1/V$ is missing there.

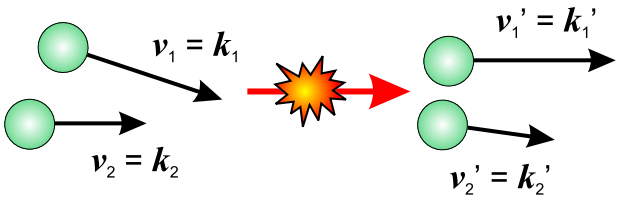

Figure 1.3.: Scattering of 2 quasifree electrons with electron velocities before and after the collision.

1.7. Remarks

- Equation (1.24) describing the contribution of the IOTs to ε is valid for slow relaxation only, that is $\Gamma \ll \omega$ [All71]. In case of fast relaxation or strong e-ph coupling, multiphonon processes have to be taken into account. The Holstein theory does so but is complicated and designed for metals with parabolic bands only [All71].

- Moreover, Eq. (1.24) considers only processes

$$|\boldsymbol{k}b\rangle \xrightarrow{\text{photon}} |\boldsymbol{k}b\rangle \xrightarrow{\text{ph, imp}} |\boldsymbol{k}'b'\rangle$$

  where the photon-related step leaves the electron in the *same* Bloch state. This is only correct when other bands are energetically separated by significantly more than the photon energy $\hbar\omega$ [Dum61].

- The case of an e-e collision is shown in Fig. 1.3. In free-electron metals with only 1 parabolic band, e-e scattering is not expected to make a significant contribution to the photon absorption in an IOT [Kav84]. First, the Coulomb interaction is effectively screened in metals. Second, wavevector conservation

$$\boldsymbol{k}_1 + \boldsymbol{k}_2 = \boldsymbol{k}_1' + \boldsymbol{k}_2' + \boldsymbol{G} \tag{1.28}$$

  and the band velocity (1.21) imply that the average velocity of the electron system does not change in an e-e collision for $\boldsymbol{G} = 0$. Only umklapp processes involving a vector $\boldsymbol{G} \neq 0$ of the reciprocal lattice can relax an electronic current.

  This situation can change in semimetals like graphite where the screening of charges is less effective due to a smaller number of electrons at the Fermi edge. Moreover, the occurence of bands with strongly differing curvature can lead to a change in the average velocity also for collisions with $\boldsymbol{G} = 0$.

  In all cases, the relaxation rate grows with electronic temperature [Kav84],

$$\Gamma^{\text{e-e}} = AT_{\text{e}}^2,$$

  because higher temperatures imply a larger number of initial and final electron states.

input x	output y	linear response function R
applied voltage V	induced current I	resistance
electric field $\boldsymbol{E}$	induced polarization $\boldsymbol{P}$	susceptibility $\chi^{(1)}$
magnetic field $\boldsymbol{B}$	induced magnetization $\boldsymbol{M}$	permeability μ
incident light field $\boldsymbol{E}_{\mathrm{inc}}$	transmitted field $\boldsymbol{E}_{\mathrm{trans}}$	sample transmittivity

Table 1.1.: Examples for perturbations x of a system and observables y which are influenced by the perturbation. The corresponding linear response functions are also shown.

1.8. Rapidly Changing Sample

Up to now, the sample was assumed to change its optical properties only little within the duration of 1 cycle $2\pi/\omega$ of the probing radiation. In TRTS, one can get quite easily beyond this quasistatic regime, for example, when a 1-THz wave with an oscillation period of 1 ps transmits a sample where free electrons decay on a 300-fs time scale. Such behavior has mainly 2 consequences:

- The quasistatic relationship (1.10) between polarization and driving field is possibly not valid any more. Therefore, the standard relations describing the wave propagation [Yeh88] are modified which is important for the extraction of the dielectric function. This problem is in principle solved; the relation between incident and transmitted THz field is, for example, given in Section 2.6.2 or in Ref. [Něm02].
- A probably more serious consequence of a quickly changing sample is that the microscopic interpretation of the dielectric function by means of the Kubo formula (1.17) is not possible any more, since this relation was derived under the assumption of a quasistatic sample [Czy04]. Therefore, knowledge of the dielectric function beyond the quasistatic regime is of somewhat limited use at present unless one can compare it to the results of explicit theoretical calculations as for example done in Ref. [Hub05b].

In the following, the general case of a linear response is considered which leads to a definition of the instantaneous spectral response and its determination in a pump-probe experiment.

1.8.1. General Linear Response

Consider a physical system which is perturbed by some "input" signal $x(t)$ and, as a consequence, changes an "output" observable $y(t)$. Examples for x and y are listed in Table 1.1. Here, the most interesting situation is, of course, a pump-probe experiment where the pump pulse triggers a rapidly evolving change in the susceptibility and transmittivity of the sample.

The relation between input and output can be formally written $y(t) = F_t[x(t')]$ where F_t is a *functional* since it has the *complete* function $x(t')$ as an argument. In many cases

the input perturbs the system considered only weakly such that one can linearize F_t with respect to $x(t')$ and obtains [Gra78]

$$y(t) = \frac{1}{\sqrt{2\pi}} \int_{-\infty}^{+\infty} \mathrm{d}t'\, R(t,t')\, x(t') \tag{1.29}$$

where $F_t(0) = 0$ was assumed without loss of generality. The response function $R(t,t') = (2\pi)^{-1/2}\delta F_t/\delta x$ is the functional derivative of F_t, and the prefactor of $1/\sqrt{2\pi}$ was introduced for consistence with the symmetric definition (B.1) of the Fourier transformation used in this work. Note that in Eq. (1.29) the complete history $t' < t$ of the input $x(t')$ contributes to the output $y(t)$ at time t. The causality principle implies that a future input does not contribute to the present output; thus one has

$$R(t,t') = 0 \quad \text{if} \quad t < t'.$$

The ultimate goal is the measurement of the response function R since it contains important information about the system investigated.

1.8.2. Instantaneous Spectral Response

Is there a quantity that describes the response properties of the sample at a certain instant of time? The answer to this question is not immediately obvious since $R(t,t')$ depends on 2 time variables. Therefore, we eliminate the time t' by a Fourier transformation (B.1) and obtain

$$y(t) = \frac{1}{\sqrt{2\pi}} \int \mathrm{d}\omega'\, R(t,-\omega')\, x(\omega')$$

where $R(t,\omega')$ is the Fourier transformed $R(t,t')$ with respect to t'. The last equation can be rewritten as

$$y(t) = \frac{1}{\sqrt{2\pi}} \int \mathrm{d}\omega'\, R_t(\omega') \cdot x(\omega') \exp(-\mathrm{i}\omega' t) \tag{1.30}$$

where

$$R_t(\omega') := R(t,-\omega') \exp(\mathrm{i}\omega' t) \tag{1.31}$$

can be interpreted as the *instantaneous spectral response* to the component $x(\omega')\exp(-\mathrm{i}\omega' t)$ of the input.

This interpretation makes sense: As will be shown below, $R_t(\omega')$ does not change with time t for a sample in a steady state; such system is often called a linear time-invariant (LTI) system [Mey97]. Time-invariant means that, if an input $x(t)$ induces an output $y(t)$, the temporally shifted input $x(t+t_0)$ will just induce the same but temporally shifted output $y(t+t_0)$. Equation (1.29) then leads to $R(t-t_0, t'-t_0) = R(t,t')$ and especially

$$R(t,t') = R(0,t'-t), \tag{1.32}$$

such that the instantaneous spectral response (1.31) becomes

$$R_t(\omega') = R(t = 0, -\omega') =: R(\omega'),$$

which does *not* depend on time t. Therefore,

$$\Xi = \left| \frac{1}{\omega' R_t(\omega')} \frac{\partial R_t(\omega')}{\partial t} \right|$$

is a measure how quickly the sample changes its linear response within 1 cycle of an input of frequency ω'.

For example, if R_t is the pump-induced change $\Delta\chi_t = (\Delta\varepsilon_t - 1)/4\pi$ in the linear susceptibility and fulfills $\Xi \ll 1$, the Kubo formula (1.17) can be used for the interpretation of χ or the dielectric function ε. In the opposite case, the Kubo formula is probably not valid any more: Its derivation assumes that the occupation numbers ρ_{mm} undergo only small relative changes within 1 optical cycle $2\pi/\omega$ [Czy04].

Before turning to an instructive example, some remarks are added:

- In frequency space, the response (1.30) reads

$$y(\omega) = \int \mathrm{d}\omega'\, R_{\omega-\omega'}(\omega') x(\omega'). \tag{1.33}$$

  and reduces to the familiar relation

$$y(\omega) = R(\omega) x(\omega) \tag{1.34}$$

  in the steady-state case because Eq. (1.32) then implies $R_{\omega-\omega'}(\omega') = R(t = 0, -\omega')\delta(\omega - \omega')$.

- The definition (1.31) of the instantaneous response agrees with that proposed in Ref. [Say94]. In this publication, the argumentation relies on the special example of a rapidly changing plasma. Here, a definition based on more general considerations is given.

- The above motivation of the instantaneous spectral response $R_t(\omega')$ started with the elimination of the time t' in $R(t, t')$ which is actually possible by any transformation $x(t') \mapsto x(\sigma')$ with respect to an orthonormal basis set $b_{\sigma'}(t')$. It can be shown, however, that the Fourier basis $b_{\omega'}(t') \propto \exp(-\mathrm{i}\omega' t')$ is the *only* basis set that results in a t-independent expression for the transformed $R_t(\sigma')$ if the sample is in equilibrium. The proof mainly shows that $\partial_t R_t(\sigma') = 0$ only and only if the Fourier basis is used.

In the following we will mainly use $R_t(\omega')$ instead of $R(t, t')$ due to its easier interpretation and since it reduces to the familiar expressions in the equilibrium case.

Example: Spectrally Flat Response

For the sake of simplicity, we assume that the instantaneous response $R_t(\omega')$ does not change over the spectrum of the input $x(t')$ which is centered at ω'_0 such that one can set $R_t(\omega') \approx R_t(\omega'_0)$. Then the response is *simply a multiplication*

$$y(t) = \mathrm{Re}\,[R_t(\omega'_0) \cdot x_{\mathbb{C}}(t)] \tag{1.35}$$

with the analytic signal $x_{\mathbb{C}}(t)$ [Die96]. The true signal $x(t)$ is just the real part of the analytic signal, $x = \mathrm{Re}\, x_{\mathbb{C}}$. Equation (1.35) implies the following points:

- Due to the modulation of the input $x(t)$ by R_t, new frequencies are created in the output $y(t)$. This effect is strong when R_t changes substantially within 1 period $2\pi/\omega'$ of the input signal, that is when $\Xi \sim 1$.
- R_t can be measured by using input pulses peaking at different times τ. For example, a delta-like input pulse $x(t) \propto \delta(t - \tau)$ yields $y(t) \propto R_\tau(\omega'_0)$. This is the principle of a pump-probe experiment.